Analytical Solution for 1-D CO_2 Injection into Aquifers with Multiple Impurities and Equilibrium Reactions

Introduction

The feed stream for underground CO_2 storage commonly contains impurities that influence multiphase flow and geochemical equilibrium in the formation. Previous experimental and numerical studies, such as Bachu and Benion (2009), have demonstrated that these impurities may separate due to chromatographic effects and change the local composition of the gas phase. However, existing analytical descriptions of the migration patterns of these components remain limited to single-impurity systems, as considered by Hosseini et al. (2012). Building on the theory of gas injection using the method of characteristics (Orr 2007) and the approach for determining intersecting key tie-lines (Yan et al., 2014), we previously developed an analytical solution for CO_2 injection into aquifers with multiple impurities for fully self-sharpening systems. The current study extends that framework to account for non-tie-line rarefactions and equilibrium reactions, such as dissociation and mineralization. Our results show that impurities more soluble than CO_2 in the initial formation fluid promote non-tie-line rarefactions. Moreover, equilibrium reactions can be incorporated into the analytical formulation using the same fundamental principles as in the non-reactive case, allowing prediction of saturation and composition profiles through apparent K-values.

Analytical solution to non-self-sharpening systems

The mass balance for one-dimensional, two-phase, multicomponent flow can be formulated as a system of first-order hyperbolic partial differential equations, corresponding to the dispersion-free limit.

$$\frac{\partial G_i}{\partial \tau}+\frac{\partial F_i}{\partial \xi}=0, \quad G_i=c_{ig}S_g+c_{iw}S_w, \; F_i=c_{ig}F_g+c_{iw}F_w$$

where G_i denotes the global concentrations of component i, and F_i represents the fractional flux of the same component. The variables τ and ξ correspond to dimensionless time and dimensionless distance in the porous medium, respectively. The term c_{ij} specifies the concentration of component i in phase j (gas g or water w), associated with saturation S_j and fractional flow f_i.

The compositional flow solution consists of tie-line paths connected by transitional ones, which appear as shocks only in fully self-sharpening systems, as addressed previously by Bagheri et al. (2026). In non-self-sharpening systems, transitions between two neighboring key tie-lines may form rarefactions. We approximate a non-tie-line rarefaction by a series of small shocks between intermediate tie-lines, as shown in Figure 1. These intermediate tie-lines can be readily constructed since they are located on the same plane spanned by the two intersecting key tie-lines.

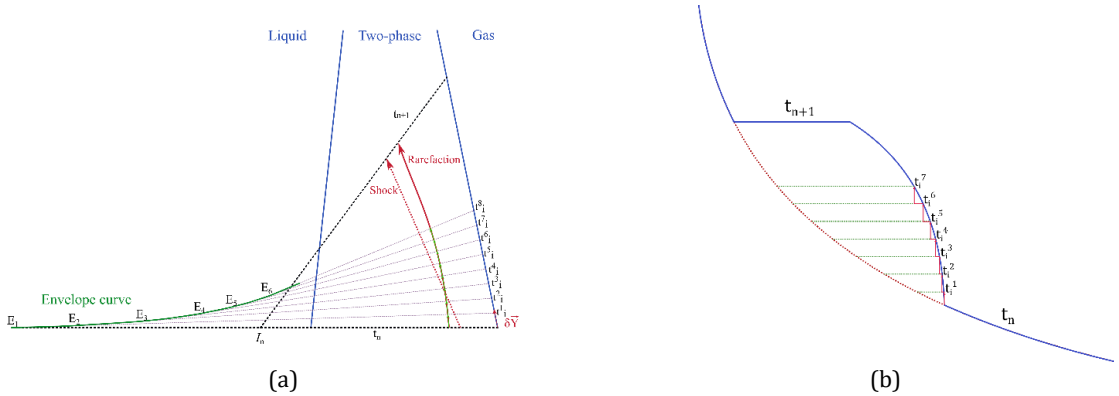

(a) (b)

Figure 1*. Construction of non-tie-line rarefaction path: a) construction of intermediate tie-lines, b) approximating rarefaction path with small jumps*

To illustrate a system with non–tie-line rarefactions, we examine the injection of CO_2 with four impurities (N_2, CH_4, SO_2, NO_2) into an aquifer initially containing 4 mol% of a single impurity gas. The injected mixture comprises 90% CO_2 and 2.5% of each impurity, with the corresponding K-values and compositions summarized in Table 1.

Table 1. *K-values for the different gas components at 200 bar and 60 °C*

Component	lnK
N_2	6.5812
CH_4	6.2158
CO_2	3.8638
H_2S	3.2563
SO_2	1.8531
NO_2	1.7643
H_2O	-4.7298

Figure 2 shows that when the initial reservoir fluid contains impurities less volatile than CO_2, evaporation of the impurity produces a non–tie-line rarefaction, whereas volatile impurities already present in the gas phase yield a fully self-sharpening solution.

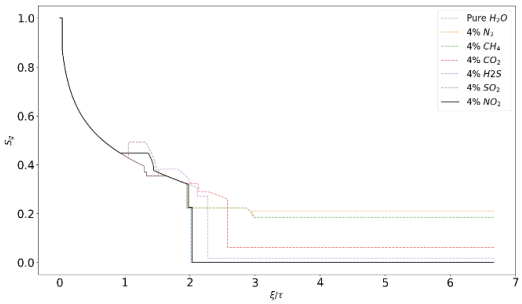

Figure 2. *Saturation profile versus for different compositions of the formation fluid.*

Effect of chemical equilibrium on propagation patterns

To investigate the effect of reactions on the propagation pattern of different gas components, the apparent equilibrium ratios were used in this study, where the apparent equilibrium ratio (K^{app}-values) is defined as:

$$K_i^{app} = \frac{y_i}{\sum x_i^{m+}}$$

where x_i^{m+} are the conjugate basic ions formed after the dissolution of gas component i. For instance, $K_{CO_2}^{app}$ is defined as:

$$K_{CO_2}^{app} = \frac{y_{CO_2}}{x_{CO_2} + x_{H_2CO_3} + x_{HCO_3^-} + x_{CO_3^{2-}}}$$

At equilibrium, the K^{app}-values depend solely on the pH of the aqueous phase, enabling the non-reactive solution to serve as an initial estimate that is then refined using K^{app}-values to obtain the reactive propagation pattern. Figure 3 presents gas saturation profiles for three scenarios—without impurities, with impurities, and with both impurities and reactions—along with the pH variation for the reactive case. The reactions and their equilibrium constant are listed in Table 2.

Table 2. *Chemical reactions and their respective equilibrium constant*

Reaction	log (K_{eq})
$H_2CO_3 \rightleftharpoons HCO_3^- + H^+$	-6.32
$HCO_3^- \rightleftharpoons CO_3^{2-} + H^+$	-10.33
$H_2SO_3 \rightleftharpoons HSO_3^- + H^+$	-1.8
$HSO_3^- \rightleftharpoons SO_3^{2-} + H^+$	-7.2
$HNO_3 \rightleftharpoons NO_3^- + H^+$	-3.2
$H_2O \rightleftharpoons OH^- + H^+$	-14.0

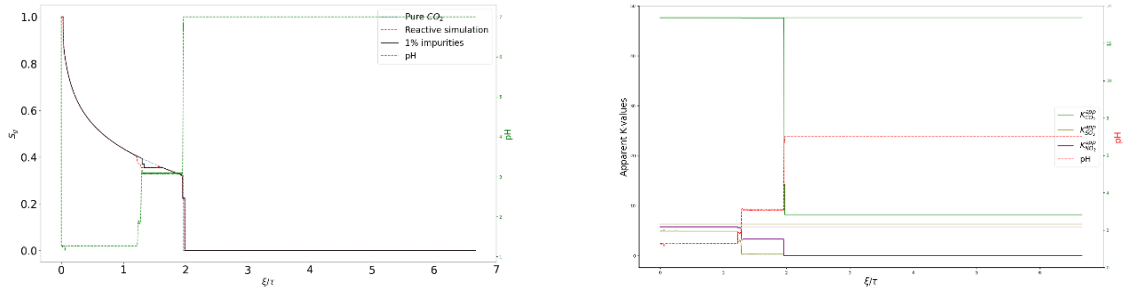

(a) (b)

Figure 3*. a) Gas saturation and aqueous pH profiles are shown for pure CO_2 without reactions, impure CO_2 without reactions, and impure CO_2 with dissociation reactions; b) corresponding K^{app}-value profiles are presented for the same cases.*

Figure 3 illustrates the pH changes in the aqueous phase during gas injection into the formation, revealing five distinct zones of constant pH. The first zone is essentially at the initial state, showing a pH of 7.0, since none of the reactive gases has arrived. The second zone forms upon the arrival of CO_2, where the pH drops to 3.3. The third zone appears with the arrival of SO_2, dropping the pH further to 1.8. Because the apparent *K*-values for NO_2 and SO_2 are very close (Figure 3(b)), the two components propagate at similar velocities, making third zone very thin in the formation and immediately followed by the fourth zone with pH 1.3. The fifth zone corresponds to the near-wellbore region, where water has evaporated and pH is no longer meaningful.

Figure 3 also compares the saturation profiles for the three cases. For pure CO_2 injection (dashed blue line in Figure 3(a)), the saturation profile is smooth, because there is only one key tie-line. In contrast, cases with more impurities show multiple-stage profiles with shocks, due to the presence of additional key tie-lines between the injection and initial fluid. Comparison between the non-reactive (solid black line) and reactive (dashed red line) shows that the propagation velocities of NO_2 and SO_2 are slightly reduced in the reactive case, due to increased dissolution in water. The K^{app}-value for these components are lower than the non-reactive *K*-values (Figure 3(b)).

Despite these minor differences, Figure 3 points out that the analytical solution for the non-reactive case can predict the main trends and key features of the reactive case.

Conclusions

This study presents a framework for modeling non–self-sharpening systems and incorporating equilibrium reactions into the one-dimensional analytical solution for component propagation during underground CO_2 storage. We demonstrate that non–tie-line rarefactions arise when the initial formation fluid contains impurities less volatile than CO_2 itself, like SO_X and NO_X. An approximation method using shock-like steps between intermediate tie-lines was proposed, demonstrating high accuracy in capturing the saturation profile.

Chemical equilibrium was also included into the analytical solution framework by introducing apparent K-values, which include the conjugate ionic forms of a dissolved gas into the traditional K-value definition. Numerical simulations indicate that the reactive solution preserves the overall structure of the non-reactive case, while pH variations highlight the influence of chemical reactions on propagation. Results show that even though the pH near the wellbore may drop as low as 1.3, the overall saturation profile remains similar to the non-reactive case, and the non-reactive analytical solution effectively captures the trend in the reactive system.

References

Bachu, S., Bennion D. B. [2009]. Chromatographic partitioning of impurities contained in a CO_2 stream injected into a deep saline aquifer: Part 1. Effects of gas composition and in situ conditions. *International Journal of Greenhouse Gas Control*, **3**, 458–467.

Hosseini, S.A.,Mathias, S.A. and Javadpour, F. [2012]. Analytical Model for CO 2 Injection into Brine Aquifers-Containing Residual CH 4. *Transport in Porous Media*, **94**(3), 795–815.

Orr, F. M. [2007]. Theory of Gas Injection Processes. *Tie-Line Publications, Copenhagen, Denmark*.

Jessen, K. [2000]. Effective Algorithms for the Study of Miscible Gas Injection Processes. *PhD dissertation, Technical University of Denmark*.

Yan, W.,Michelsen, M.L. and Stenby, E.H. [2014]. Negative flash for calculating the intersecting key tielines in multicomponent gas injection. *Industrial and Engineering Chemistry Research*, **53**(36), 14094–14112.